Embryonic endothelial progenitor cells armed with a suicide gene target hypoxic lung metastases after intravenous delivery

Jiwu Wei,[1] Sabine Blum,[2] Marcus Unger,[1] Gergely Jarmy,[1] Mathias Lamparter,[2] Albert Geishauser,[2] Georgios A. Vlastos,[2] Gordon Chan,[3] Klaus-Dieter Fischer,[3] Dirk Rattat,[4] Klaus-Michael Debatin,[1] Antonis K. Hatzopoulos,[2,*] and Christian Beltinger[1,*]

[1]University Children's Hospital, Ulm D-89075, Germany
[2]GSF-National Research Center for Environment and Health, Munich D-81377, Germany
[3]Department of Physiological Chemistry
[4]Department of Nuclear Medicine
University of Ulm, Ulm D-89081, Germany
*Correspondence: christian.beltinger@medizin.uni-ulm.de (C.B.), hatzopoulos@gsf.de (A.K.H.)

Summary

We show that mouse embryonic endothelial progenitor cells (eEPCs) home preferentially to hypoxic lung metastases when administered intravenously. This specificity is inversely related to the degree of perfusion and vascular density in the metastasis and directly related to local levels of hypoxia and VEGF. Ex vivo expanded eEPCs that were genetically modified with a suicide gene specifically and efficiently eradicated lung metastases with scant patent blood vessels. eEPCs do not express MHC I proteins, are resistant to natural killer cell-mediated cytolysis, and can contribute to tumor vessel formation also in nonsyngeneic mice. These results indicate that eEPCs can be used in an allogeneic setting to treat hypoxic metastases that are known to be resistant to conventional therapeutic regimes.

Introduction

The growth and metastasis of solid tumors correlate with their ability to induce formation of new blood vessels. In addition to sprouting angiogenesis from neighboring resident endothelial cells, tumors also build vessels by recruitment and in situ differentiation of circulating endothelial progenitor cells (Hanahan and Folkman, 1996; Asahara et al., 1997, 1999; Shi et al., 1998; Peichev et al., 2000; Gehling et al., 2000; Lyden et al., 2001; Reyes et al., 2002). Bone marrow-derived endothelial precursors are necessary and sufficient for tumor angiogenesis (Lyden et al., 2001), and EPCs differentiated ex vivo from multipotent adult progenitor cells home to tumors (Reyes et al., 2002). Irradiation followed by bone marrow transplantation of unfractionated bone marrow cells (Davidoff et al., 2001), endothelial progenitor-like cells (Ferrari et al., 2003), or tie-2^+ myeloid progenitors (De Palma et al., 2003), which were engineered to hinder angiogenesis, slows growth of posttransplant tumor challenges. Genetically modified $CD34^+$ cells also homed to angiogenic sites in a rhesus monkey model and exerted a bystander effect in vitro (Gomez-Navarro et al., 2000). These findings offer the possibility to exploit EPCs for cancer therapy (Asahara et al., 1999). However, the utility of bona fide, ex vivo expanded EPCs for this purpose without prior bone marrow transplant is yet unknown.

The potential of eEPCs to serve as cellular vehicles to target cancers depends on efficient and specific (ex vivo) gene transfer and the ability to stably carry therapeutic loads through the blood stream to the intended target. What renders EPCs an attractive candidate cellular vehicle is that they may home exclusively to sites of active neovasculogenesis. Because cancers most often kill by metastases, it is crucial to evaluate the efficacy of EPCs for cancer therapy in metastatic models. Thus, knowledge of the differential homing of EPCs to metastases of different size, in different organs, in different locations within a tissue, as well as to normal organs, is essential, but not available.

The study of adult endothelial progenitor cells is in early stages and under intense debate (Rafii and Lyden, 2003; Patterson, 2003). Adult stem cells are difficult to isolate and maintain in vitro, which diminishes availability and thus the prospects of systematic molecular studies and genetic manipulation. One

SIGNIFICANCE

The contribution of endothelial progenitor cells to tumor neoangiogenesis opens new ways to hinder tumor growth. We found that embryonic endothelial progenitor cells (eEPCs) show a remarkably efficient and specific affinity for disseminated lung metastases without the need of prior irradiation and bone marrow transplantation. They particularly targeted hypoxic lung metastases that are often resistant to chemotherapy or radiation therapy. Homing of eEPCs to normal tissues was low and without adverse effects or formation of teratocarcinomas. eEPCs can be expanded indefinitely, are easy to manipulate ex vivo, and appear to be immunoprivileged. Taken together, these results suggest that embryonic EPCs constitute clinically relevant cellular vehicles for systemic gene therapy of lung metastases.

exciting alternative are the embryonic endothelial progenitor cells (eEPCs) isolated from mouse embryos or derived from differentiation of embryonic stem cells (Hatzopoulos et al., 1998; Levenberg et al., 2002; Yurugi-Kobayashi et al., 2003; Marchetti et al., 2002). Embryonic EPCs possess distinct advantages: they grow in unlimited fashion, proliferate rapidly, and are easily amenable to genetic manipulation (Hatzopoulos et al., 1998). It was recently shown that embryonic EPCs retain their ability to incorporate into vascular networks in active sites of angiogenesis in the adult (Yurugi-Kobayashi et al., 2003; Vajkoczy et al., 2003). It is yet unknown, though, whether eEPCs possess a different therapeutic potential than adult EPCs. Based on these properties, we investigated the homing and therapeutic utility of mouse eEPCs armed with a suicide gene in syngeneic and nonsyngeneic lung metastasis models without bone marrow transplantation.

Results

eEPCs do not express MHC I, are resistant against nonactivated NK cells, and form tumor vessels in nonsyngeneic mice

An advantage for cell-based therapeutic approaches would be donor material that is not rejected by the host's immune system. Cells isolated from early embryonic stages such as the eEPCs might possess such properties, because early embryonic tissue evades the maternal immune system until the immunological barrier between mother and fetus is established. Therefore, we examined whether the eEPCs isolated at E7.5 possess molecular features that allow them to evade rejection when transplanted in nonsyngeneic mice.

MHC I surface antigens determine the response of cytotoxic T cells against allogeneic cells. We determined the level of MHC I expression on eEPCs using a pan anti-MHC class I antibody. FACS analysis indicated that MHC I antigens were not expressed on three eEPC clones isolated independently from C57BL/6 mice, whereas control fibroblasts, T cells, and mast cells from this strain showed strong antibody binding (Figure 1A). This result suggests that eEPCs are protected against T cell-mediated immune responses.

Because rejection of transplants is also determined by sensitivity toward NK cells, we tested whether NK cells can target the MHC I-negative eEPCs. To assess spontaneous NK cell cytotoxicity against eEPCs, we performed cell lysis assays using T cell-depleted splenocytes derived from C3H mice. As positive and negative controls, we used YAC-1 and RMA/S, respectively, as target cell lines. YAC-1 cells are derived from A/Sn mice and are sensitive to C3H-derived NK cell-mediated spontaneous cytotoxicity. In contrast, the MHC class I-deficient RMA/S cells, derived from C57BL/6 mice, are resistant. We found that YAC-1 cells were readily lysed in the presence of freshly isolated NK effectors, while eEPCs were resistant to NK cells similar to RMA/S cells, suggesting that eEPCs do not engage activating NK receptors (Figure 1B). The escape of early surveillance by NK cells coupled to the lack of MHC I antigens may allow recruitment and persistence of eEPCs in nonsyngeneic hosts.

To test this notion, LM8 osteosarcoma cells (which are derived from C3H mice of H-2K^k haplotype) were mixed with DiI (1,1′-dioctadecyl-3,3,3′3′-tetramethylindocarbocyanine perchlorate)-labeled eEPCs from 129Sv, C57/BL/6, or FVB mice (H-2K^b, H-2K^b, and H-2K^q haplotypes, respectively) and transplanted subcutaneously into C3H mice. This experimental setup, as compared to intravenous (i.v.) injection of eEPCs into tumor-bearing mice, allowed longer observation periods and increased the number of eEPCs contributing to blood vessel formation, thus facilitating evaluation of eEPC survival. Tumor growth was followed for up to 24 days before FITC-labeled HPA lectin was injected intravenously to decorate tumor vessels 5 min prior to tumor isolation. Tumors were examined by whole-mount fluorescence microscopy. Nearly all eEPCs in the visible tumor periphery had incorporated into tumor vessels, and 20%–25% of the tumor vasculature was composed of DiI-positive eEPC-derived cells (Figure 1D), indicating that eEPCs survive and build tumor vessels in nonsyngeneic hosts.

Tail vein-injected eEPCs are sequestered mainly in the lung and spleen

The effectiveness of eEPCs as a cellular vehicle for tumor therapy depends on normal tissue being spared by eEPCs. We therefore quantitatively determined the distribution and fate of eEPCs in various organs of tumor-free mice after tail vein injection of cells loaded with ^{111}Indium (In)-labeled low-density lipoprotein (LDL). The efficacy of LDL-particle uptake by eEPCs was assessed in parallel experiments using DiI-labeled LDL. DiI-labeled LDL was readily and uniformly taken up and retained by eEPCs. Similarly, there was no leakage of radioactive label into the medium after 48 hr of cell culture of eEPCs labeled with ^{111}In-LDL, and the radioactive labeling did not affect cellular morphology or proliferation rates (data not shown). Cell-free ^{111}In-labeled LDL is taken up predominantly by the liver (Virgolini et al., 1991), whereas small fragments of ^{111}In-DTPA (diethylenetriaminepenta-acetic acid)-LDL and ^{111}In-DTPA are excreted by the kidneys (Rogers et al., 1995). Thus, except for liver and kidneys, radioactivity in organs represented the presence of eEPCs.

After tail vein injection into C3H mice, eEPCs were sequestered predominantly in the lung and the spleen (Figure 2A). Sequestration of eEPCs in liver and kidneys was low, considering that activity in these organs may also represent label being excreted. There were no measurable counts in gut, brain, empty bladder, bone, or bone marrow. Organ-specific radioactivity decreased over time, and radioactivity was detected in the cage bedding consistent with sequestered eEPCs being destroyed and cell-free label being excreted into urine and stool.

We confirmed and extended the biodistribution data by immunohistochemistry analysis. eEPCs marked with enhanced green fluorescent protein (EGFP) were present in low numbers in the lung and spleen of C3H mice while rare eEPCs were detected in liver and brain and no eEPCs were found in the kidneys and in the bone marrow (Figure 2B and data not shown). Taken together, these data show that sequestration leads to a low-density distribution of tail vein-injected eEPCs predominantly in lung and spleen that diminishes over time.

Tail vein-injected eEPCs home specifically and efficiently to metastases in the lung

Next we wanted to know whether eEPCs home to tumors and which tumor characteristics influence homing. We investigated the homing of eEPCs in two mouse models of multiple metastases using the LM8 osteosarcoma cell line that creates metastases in lung, liver, and kidneys and the Lewis lung carcinoma (LLC) cells that form metastases only in the lung. We injected

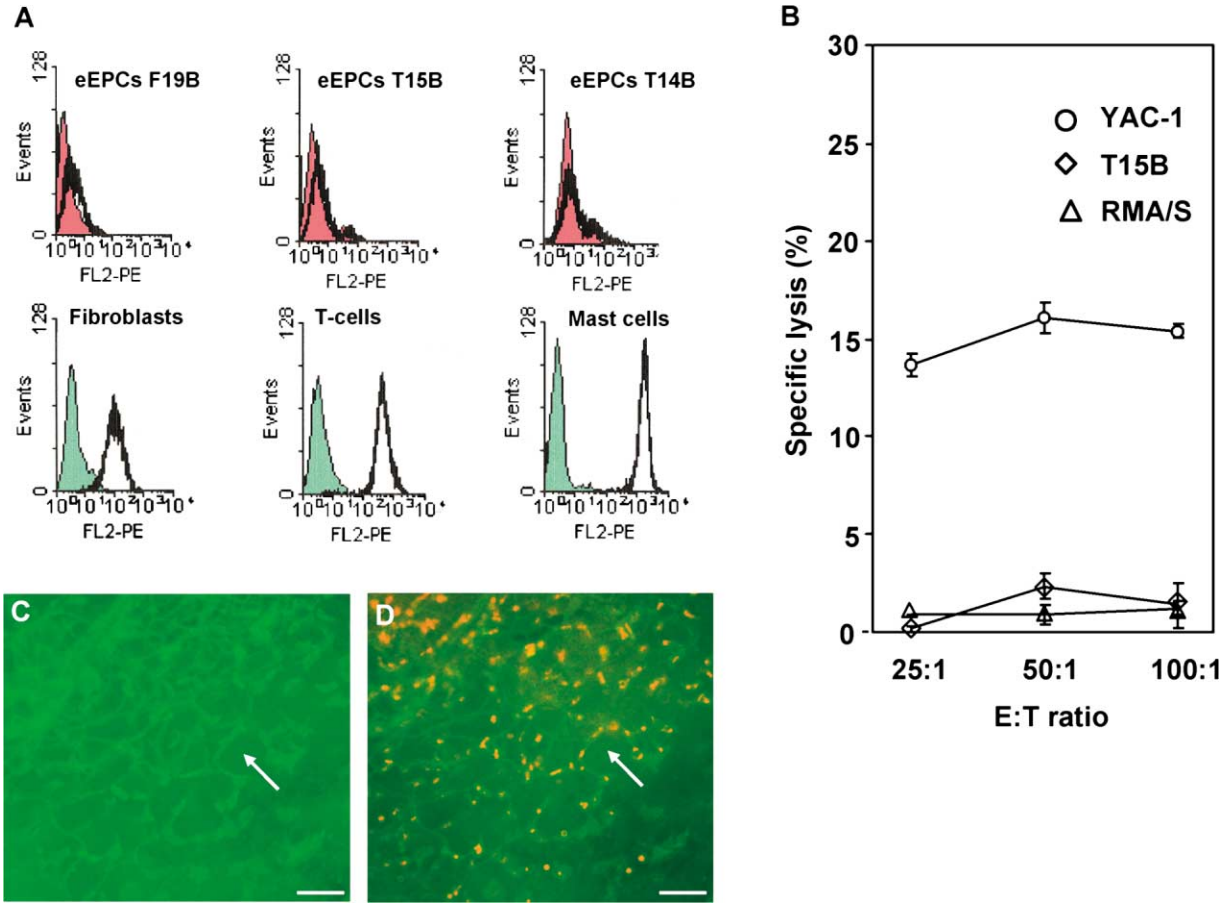

Figure 1. eEPCs are immunoprivileged

A: FACS analysis using a pan anti-mouse MHC I antibody shows no MHC I expression in three independently isolated eEPC clones, F19B, T15B, and T14B. NIH 3T3 fibroblasts, T cells, and primary mouse mast cells display high MHC I levels and were used as positive controls.

B: eEPCs are resistant to nonactivated NK cells. Freshly purified splenocytes depleted of $CD4^+$ and $CD8^+$ cells were used as effectors (E) in a standard ^{51}Cr-release assay against the following target cells (T): YAC-1 (sensitive to spontaneous NK cells), RMA/S (resistant to NK cells), and TI5B (an eEPC cell line). Results are representative of two independent experiments.

C and D: eEPCs form tumor vessels in nonsyngeneic mice. DiI-labeled eEPCs from C57/BL/6 mice were subcutaneously cotransplanted with LM8 cells in a ratio of 1:20 into C3H mice. After 24 days of tumor growth, mice were injected i.v. with HPA-FITC-lectin to decorate perfused tumor vessels before tissue isolation. Whole-mount tumor specimens were examined by fluorescence microscopy. Arrows point to the same areas for orientation. Scale bars represent 150 μm.

C: HPA-FITC-lectin decorated tumor vessels (green color).

D: Incorporation of DiI-labeled eEPCs (orange) into the tumor vasculature (green).

LM8 cells by tail vein injection in C3H mice (syngeneic to LM8 cells) and LLC cells in C57BL/6 mice (syngeneic to LLC cells). Fourteen days later, we transplanted into both tumor models eEPCs isolated from C57BL/6 E7.5 embryos and marked either by DiI or by stable EGFP expression. Consequently, the eEPCs were syngeneic in the LLC-carrying mice and allogeneic in the LM8-bearing mice.

Five to seven days after tail vein injection of DiI-labeled eEPCs or eEPCs expressing EGFP in mice with LM8 metastases in the lung, liver, and kidneys, histological analysis showed that eEPCs homed into most metastases in the lung (Figures 3A–3D) and with low frequency into liver and kidney metastases (Figure 3E). Thus, when given via the tail vein, eEPCs appear to home to lung metastases in a first pass effect but far less efficiently to metastases downstream of the lung.

Parallel experiments using mice carrying LLC metastases in the lung showed similar results (Figure 3F). In both tumor types, homing was specific within the metastases, since very few eEPCs were found in the surrounding normal lung tissue at this time point (Figures 3A–3F). Homing was also efficient with numerous eEPCs present within the tumor nodules.

To further quantify eEPC homing, the lungs of six mice with LM8 metastases, which received EGFP-transfected eEPCs twice spaced 3 days apart, were sectioned in 4 μM intervals and the presence of eEPCs was determined by immunohistochemistry using an antibody against EGFP. eEPCs were found in 77% of all lung metastases with a range of 67% to 100% (see Supplemental Table S1 at http://www.cancercell.org/cgi/content/full/5/5/477/DC1). eEPCs were also present in 2 out of 17 liver metastases and in 1 out of 6 kidney metastases. Experiments in three mice carrying LLC tumors in the lung showed homing to 90% of the metastases.

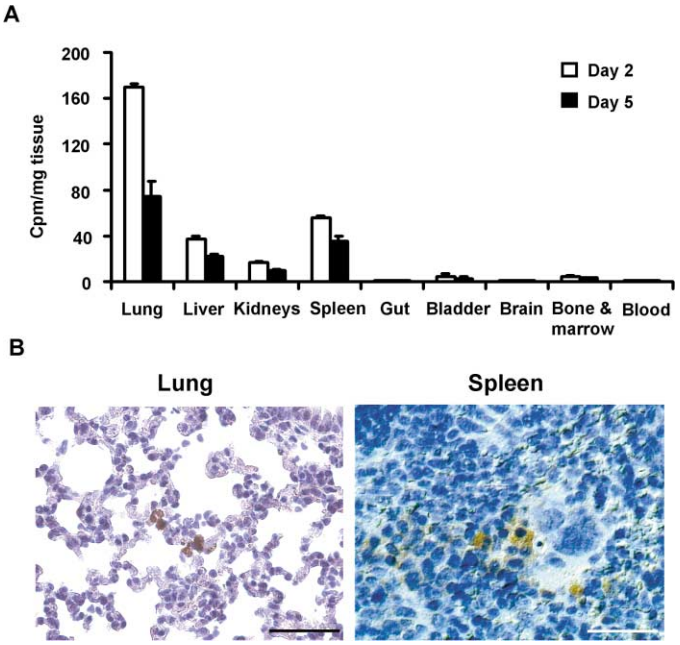

Figure 2. Transient and low-level distribution of eEPCs in normal organs following tail vein injection

A: ^{111}In-LDL-labeled eEPCs were injected into the tail vein of C3H mice and organs were procured and analyzed using a γ counter on days 2 (n = 3) and 5 (n = 3) after injection. Background activity was subtracted, and organ-specific levels of radioactivity were calculated as activity per mg of organ mass. The means and standard deviations are depicted. Similar results were obtained in two independent experiments.
B: EGFP-labeled eEPCs were injected into the tail vein of C3H mice. Organs were isolated 2 days later and eEPCs were detected by immunohistochemistry using an anti-EGFP antibody (brown staining) in lung and spleen. Scale bars represent 50 μm.

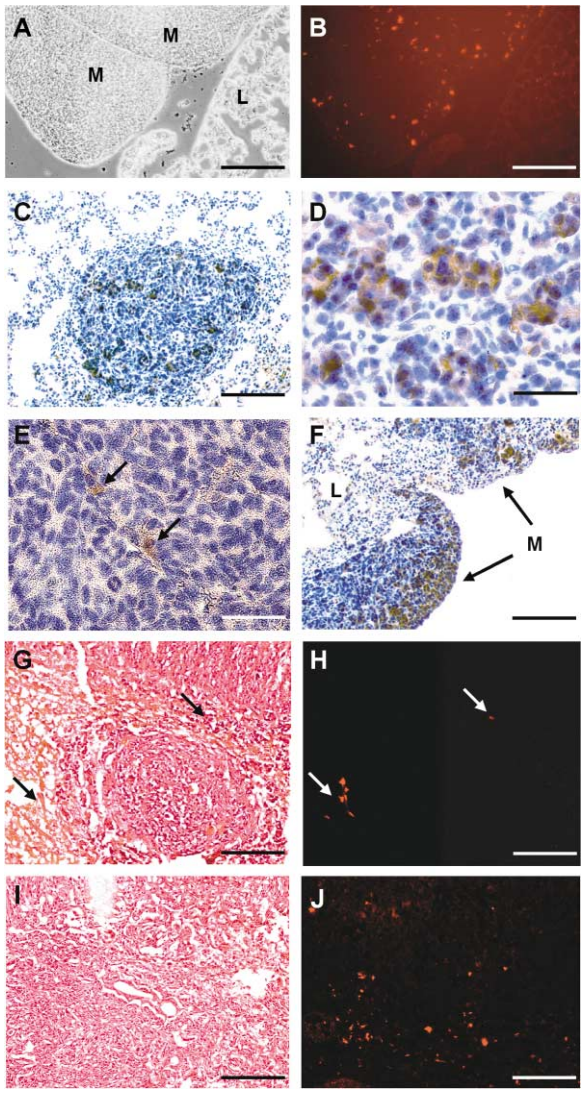

Figure 3. Tail vein-injected eEPCs specifically home to metastases mainly in the lung

LM8 or LLC cells were injected into the tail vein of C3H or C57/BL/6 mice, respectively. After metastases had formed, DiI- or EGFP-labeled eEPCs or fibroblasts were injected i.v. Following organ procurement, the injected cells were detected by DiI fluorescence or by immunohistochemistry using an anti-EGFP antibody.
A and B: DiI-labeled eEPCs home to LM8 lung metastases. Organs were secured 7 days after injection of eEPCs. Numerous eEPCs are present in subpleural metastases (M) but not within adjacent lung tissue (L).
C and D: EGFP-labeled eEPCs home to LM8 lung metastases. eEPCs were injected i.v. twice spaced 3 days apart and organs were secured 5 days later. Numerous eEPCs (brown staining) are seen in a metastasis but not in adjacent normal tissue. **D** is a higher magnification of **C**.
E: Low numbers of eEPCs (brown staining; arrows) home to LM8 metastases in liver tissue of mice generated as described in **C** and **D**.
F: EGFP-labeled eEPCs home to LLC lung metastases. Mice received two injections of eEPCs spaced 3 days apart and lungs were procured 5 days later. eEPCs home to LLC metastases in the lung (M, arrows) but not to adjacent lung tissue (L).
G–J: Fibroblasts do not home to LLC metastases. Mice were injected once with DiI-labeled fibroblasts or eEPCs and lungs were retrieved 2 days later. No fibroblasts are seen in the metastases, while some are found in the lung parenchyma (**G** and **H**; arrows point to the same area for orientation). In contrast, numerous eEPCs have homed into a metastasis (**I** and **J**; the inside of a large metastasis is depicted). **G** and **I** are H&E stains.
Scale bars represent 200 μm (**A**–**C**, **F**–**J**) and 50 μm (**D** and **E**).

Taken together, homing in lung metastases was independent of the eEPC labeling technique, the tumor type, and the location of the metastases in the lung, and it was comparable in both syngeneic and nonsyngeneic mice. To exclude unspecific sequestration as a major cause of eEPC delivery to the metastases, we performed parallel experiments with DiI-labeled fibroblasts, which are of similar size as the eEPCs (20–25 μM). Histological examination of lung tissue of LLC-bearing mice 2 days after i.v. cell injection showed that similar numbers of eEPCs and fibroblasts were present within normal lung tissue. In contrast, we observed no or only occasional fibroblasts within tumor nodules, whereas at the same time point there was an abundance of tumor-embedded eEPCs (Figures 3G–3J). Thus, while sequestration in the lung was comparable for both cell types, efficient homing to metastases was a specific property of eEPCs.

Lung metastases with impaired vascular function preferentially recruit eEPCs

We observed that in both the LM8 and LLC tumor models, not all metastases in the lung recruited eEPCs (Figures 4A and 4B). We therefore examined whether size, vascular density, and localization of the metastases influence homing of eEPCs.

Histological analysis of recruiting and nonrecruiting large LM8 tumor nodules localized in subpleural areas showed that

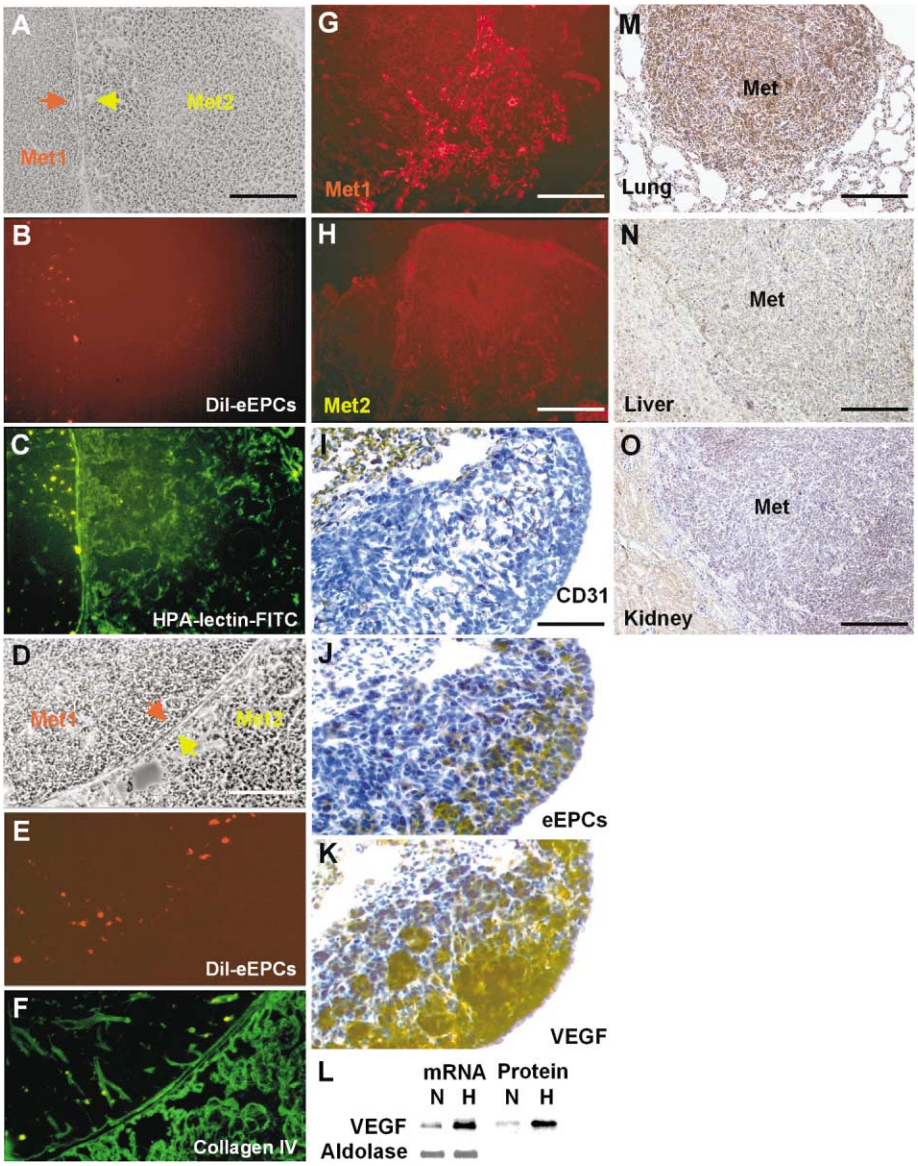

Figure 4. Lung metastases with impaired vascular function preferentially recruit eEPCs

A–H: LM8 cells were injected into the tail vein of C3H mice, and DiI-labeled eEPCs were given once by tail vein 14 days later. Seven days later, organs were retrieved and cryosectioned for fluorescence microscopy to visualize the DiI-labeled cells.

A–C: eEPCs preferentially home to poorly perfused metastases. Five to seven minutes before organ isolation, HPA-FITC-labeled lectin was injected i.v. to decorate perfused blood vessels. Phase contrast microscopy of lung sections (A) shows two adjacent metastases (Met1 and Met2) separated by pleural lining (arrows). Fluorescence microscopy revealed homing of DiI-labeled eEPCs into Met1 only (**B**), correlating with less perfused tumor vessels as visualized by binding of HPA-FITC lectin to endothelial cells (**C**).

D–F: Phase contrast microscopy (**D**) delineates the two adjacent metastases Met1 and Met2 (the pleural demarcation is outlined by arrowheads). DiI-labeled eEPCs are present only in Met1 (**E**) that is less vascularized as shown by anti-collagen IV antibody labeling (**F**).

G and H: Metastases recruiting eEPCs show high VEGF expression. LM8 metastases Met1 (which recruits eEPCs) and Met2 (which does not) were stained with anti-VEGF antibody.

I–K: Both tumor cells and homed eEPCs express VEGF. LLC cells were injected into the tail vein of C57/BL/6 mice. Fourteen days later, eEPCs expressing EGFP were given twice spaced 3 days apart. Two days after the second eEPC injection, lungs were retrieved and sectioned. Blood vessels were detected by anti-CD31 antibody (**I**), eEPCs by anti-EGFP antibody (**J**), and VEGF-producing cells by anti-VEGF antibody (**K**). A poorly vascularized metastasis (**I**) recruits many eEPCs (**J**) and stains positive for VEGF in most of its expanse (**K**), including areas that stained positive for EGFP in **J**.

L: Hypoxia upregulates VEGF mRNA and protein in eEPCs. eEPCs were subjected to normoxia or hypoxia for 6 hr. VEGF mRNA was detected by RT-PCR with aldolase used as control. VEGF protein was immunoprecipitated and detected by Western blotting.

M–O: Liver and kidney LM8 metastases express less VEGF than lung metastases. Five metastases each in the lung, liver, and kidneys from two mice were stained for VEGF by immunohistochemistry. Representative staining of metastases in the lung (**M**), liver (**N**), and kidneys (**O**) are shown.

Scale bars represent 200 μm (**A–C**, **G**, **H**, **M–O**), 150 μm (**D–F**), and 100 μm (**I–K**).

eEPCs were predominantly found in poorly perfused metastases as revealed by i.v. premortem HPA-FITC-lectin injection (Figures 4A–4C). The hypoperfused metastases were also hypovascularized, as was determined by postmortem staining for collagen IV that is localized in the endothelial basal membrane of blood vessels (Figures 4D–4F). There was no difference in the ratio of well-vascularized to poorly vascularized metastases between eEPC-injected and noninjected tumor-bearing mice, indicating that recruited eEPCs did not block blood flow in the metastases. Instead, these observations indicated that eEPCs preferentially home to those metastases where decreased vascularity has led to decreased perfusion. Further analysis revealed that poorly vascularized subpleural metastases recruiting eEPCs in their periphery stained heavily for VEGF in their central areas, whereas nonrecruiting metastases did not (Figures 4G and 4H).

We extended our investigation to smaller LM8 and LLC metastases using immunohistochemistry. Analyzing 14 LM8 metastases in 3 C3H mice and 15 LLC metastases in 3 C57/BL/6 mice, we confirmed that eEPCs, detected by anti-EGFP antibody, were preferentially found in metastases with decreased vascularity in both tumor models, as visualized by anti-CD31 antibody staining (Figures 4I and 4J). Surprisingly, we found that in some of these smaller metastases, VEGF expression colocalized not only with tumor cells but also with eEPCs (Figure 4K). In vitro, eEPCs express low levels of VEGF in normoxic conditions but upregulate both VEGF mRNA and protein under hypoxic conditions (Figure 4L). These data indicate that eEPCs might home preferentially to hypovascular metastases suffering from hypoxia, which then causes upregulation of VEGF in tumor cells and recruited eEPCs.

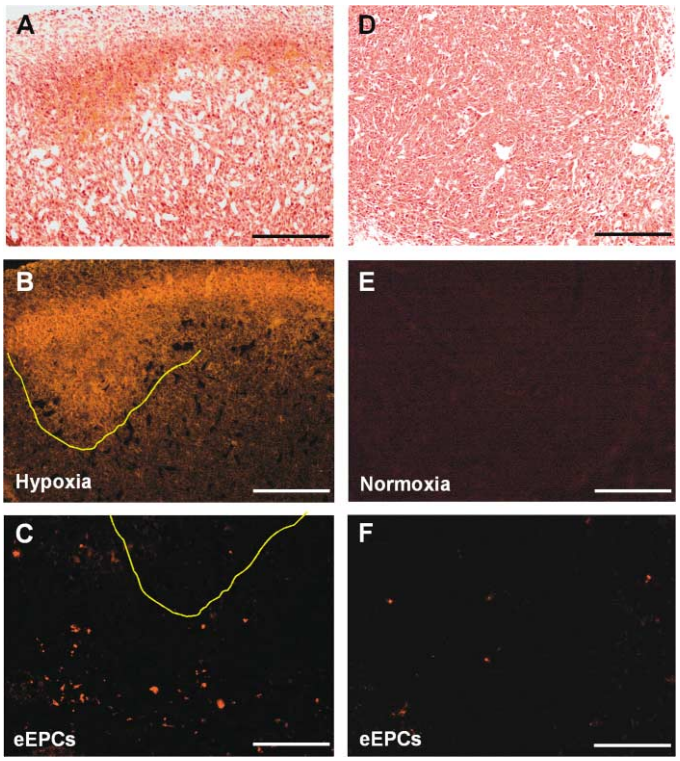

Figure 5. eEPCs home preferentially to hypoxic metastases

Two days after tail vein injection of 4 × 10^5 DiI-labeled eEPCs into mice bearing LLC metastases, animals were injected premortem with the hypoxia-sensitive compound pimonidazol. Bound pimonidazol was visualized postmortem by immunofluorescence detection using an anti-pimonidazol antibody, while eEPCs were detected by DiI fluorescence.
A–C: A hypoxic metastasis recruits many eEPCs in the tumor tissue adjacent to the hypoxic area.
D–F: A normoxic metastasis recruits few eEPCs.
A and **D** are H&E stainings. Scale bars represent 200 μm.

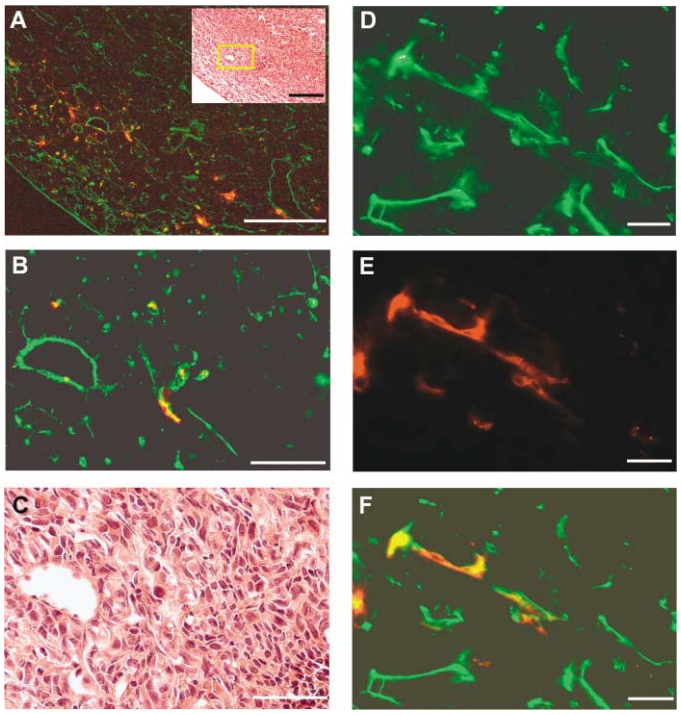

Figure 6. eEPCs incorporate long-term into tumor vessels

14–17 days after tail vein injection of DiI-labeled eEPCs into mice bearing LLC metastases, the lungs were examined by fluorescence and light microscopy. Tumor vessels were stained with FITC-labeled Isolectin B_4.
A: eEPCs (red) have homed predominantly to the periphery of a large metastasis. The insert shows the H&E stain of the same area.
B and C: Larger magnification corresponding to the boxed area in **A**. A number of eEPCs (red) have incorporated (yellow and orange) into tumor vessels (green).
C: H&E stain of **B**.
D–F: eEPCs incorporated also in blood vessels closer to the tumor's center.
D: Endothelial cells (green) stained with FITC-labeled Isolectin B_4.
E: DiI-labeled eEPCs (red) in the area corresponding to **D**.
F: Overlay of **D** and **E** shows that eEPCs have incorporated (orange and yellow) into tumor vessels (green).
Scale bars represent 200 μm (**A**), 50 μm (**B** and **C**), and 20 μm (**D–F**).

To test this notion, we determined the hypoxia levels in tumor tissue by premortem injection of pimonidazol (which binds to hypoxic tissue only) followed by immunofluorescence detection using an anti-pimonidazol antibody. Hypoxic metastases typically recruited many eEPCs around their hypoxic areas (Figures 5A–5C). In contrast, metastases that were negative for pimonidazol staining and not hypoxic recruited only very few eEPCs (Figures 5D–5F).

eEPCs incorporate long-term into tumor vessels

To determine if eEPCs contribute long-term to tumor vessel formation, DiI-labeled eEPCs were injected into the tail vein of mice bearing LLC metastases. Analysis 14–17 days later showed that eEPCs had integrated into 1%–5% of the tumor vessels of a given metastasis and that the majority of eEPCs were localized in the tumor tissue proper (Figure 6). In the LM8 model, we calculated that 4%–7% of tumor blood vessels in the recruiting lung metastases contained eEPCs at 10 days after eEPC injection (Figures 4C and 4F and data not shown).

Effective target and bystander killing by CD/5-FC in eEPCs

To target lung metastases, we chose a suicide gene system because it allows for inducible cell death, giving time for the eEPCs to home to, integrate into, and proliferate within the metastases before triggering their death. For this purpose, we stably transfected eEPCs with the yeast cytosine deaminase (CD) gene fused to uracil phosphoribosyl transferase (UPRT, which shortcuts rate-limiting enzymatic steps). The fusion gene acts as a strong catalyst converting the harmless prodrug 5-fluorocytosine (5-FC) to the cytotoxic compound 5-fluorouracil (5-FU) (Chung-Faye et al., 2001), a drug widely used in clinical practice. 5-FU diffuses into the interstitial space and is taken up by surrounding cells, thus exerting a strong bystander cytotoxic effect (Huber et al., 1994).

eEPCs carrying the fusion gene (eEPC-CD), but not eEPCs containing the empty control vector, were effectively killed by 5-FC concentrations achievable in vivo (Figure 7A). 5-FC-mediated cytotoxic effects were at maximum level after 5 days, when near-complete cell death occurred (Figure 7B). Since eEPCs were located predominantly within tumor tissue proper, we first determined the bystander cytotoxic effect of eEPC-CD on LM8 osteosarcoma cells. Mixtures of eEPCs and LM8 cells were treated with 5-FC. Cell survival less than the percentage of LM8

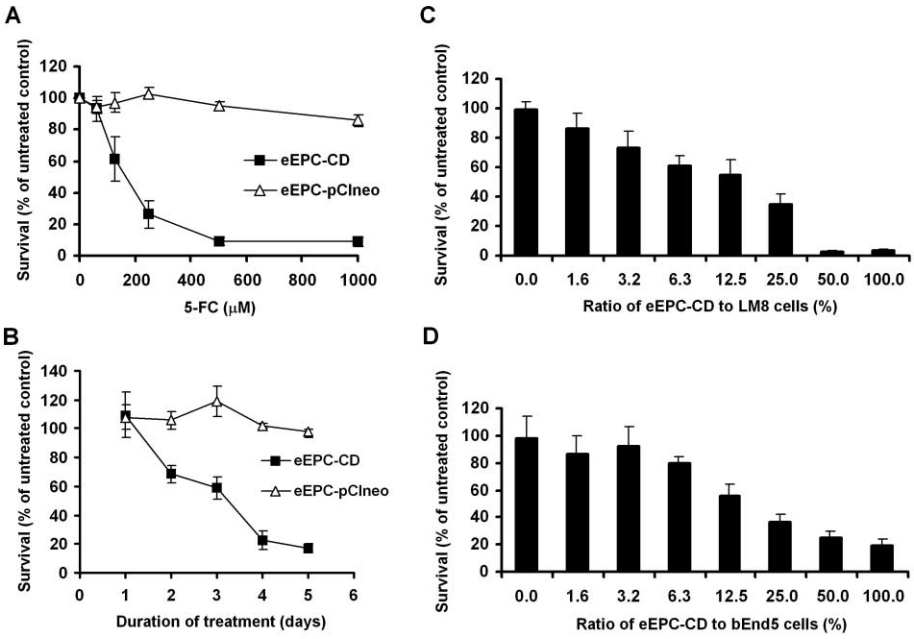

Figure 7. Effective target and bystander killing by CD/5-FC in eEPCs

A: eEPC-CD are killed by 5-FC depending on dose. eEPC-CD or eEPC-pCIneo (empty vector control) cells were treated for 5 days with 5-FC in doses as indicated.

B: Killing of eEPC-CD by 5-FC is protracted. eEPC-CD/UPRT or eEPC-pCIneo cells were exposed to 500 μM 5-FC for the time indicated.

C: eEPC-CD with 5-FC exert a bystander effect on tumor cells. Mixtures of eEPC-CD cells with LM8 cells in the ratios indicated were treated with medium alone (control) or with 1 mM 5-FC for 5 days.

D: eEPC-CD with 5-FC exert a bystander effect on microvascular endothelial cells. Mixtures of eEPCs with bEnd5 cells in the ratios indicated were treated with medium alone (control) or with 1 mM 5-FC for 5 days. In all cases, survival was measured by the MTT test. Results are means of quadruplicates and are expressed as the percentage of untreated controls. Similar results were obtained in three independent experiments.

cells put into the assay denotes bystander killing. For instance, we measured that cell survival in a mixture containing 6.25% eEPC-CD was just 60% (instead of the 93.75% expected if only eEPC-CD were killed), demonstrating a bystander effect (Figure 7C). In parallel experiments, we investigated the bystander effect of eEPC-CD on the mouse microvascular endothelial cell line bEnd5 that served as a surrogate for tumor endothelial cells. Similar to the effect on tumor cells, eEPC-CD exerted a bystander cytotoxic effect on bEnd5 cells (Figure 7D).

eEPC-CD with 5-FC prolong life of mice with lung metastases

We then investigated the effectiveness of eEPC-CD to kill tumor cells in vivo. Knowing that eEPCs injected into the tail vein home predominantly to metastases in the lung, we selected LLC as the tumor metastasis model. Injection of the tumor cells into the tail vein led to formation of numerous lung metastases in each mouse, creating a hard-to-treat experimental system. Mice with established multiple lung metastases lived significantly longer when eEPC-CD were given by tail vein injection followed by systemic 5-FC administration (Figure 8A). Interestingly, metastases-bearing mice that received eEPC-CD without 5-FC lived shorter. Because eEPCs injected into mice without metastases did not shorten survival, the decreased survival in tumor-bearing mice cannot be attributed to a toxic effect of the eEPC-CD, suggesting instead that eEPC-CD without 5-FC treatment increased tumor growth.

Similar results were also obtained using LM8 osteosarcoma cells in C3H mice (data not shown). Survival rates were lower as compared to the LLC experiments because of metastases growing also in liver and kidneys, organs that were not efficiently reached by eEPC-CD injected into the tail vein.

The surviving control mice without tumor implantation that received eEPCs i.v. were analyzed 3 months later. Inspection of organs did not reveal visible toxic effects or embryonic tumors.

eEPC-CD with 5-FC eradicate hypovascular metastases

In the mice that had received eEPC-CD and 5-FC, the metastases at the time of death were strikingly fewer than in the control untreated mice (Figures 8B and 8D). The remaining metastases that escaped treatment were highly vascularized (Figures 8D and 8E) as compared to control untreated animals where the majority of the metastases were poorly vascularized (Figures 8B and 8C). This is in line with the finding that eEPCs home preferentially to less vascularized metastases and is consistent with the notion that these metastases are eradicated following 5-FC administration, leaving only the more vascularized metastases to grow further.

Discussion

In cancer patients with no wounds or uterine cycling, neovasculogenesis is restricted to growing tumor masses, and therefore recruitment of endothelial progenitors promises to be specific to the tumor. Furthermore, since neovasculogenesis is a universal feature of most tumor types, exploiting it to recruit therapeutic EPCs offers the potential of targeting tumors irrespectively of their antigenic and genetic make-up. Genetically modified endothelial progenitor cells have been used successfully for this purpose (Gomez-Navarro et al., 2000; Davidoff et al., 2001; Ferrari et al., 2003; De Palma et al., 2003). Differentiated endothelial cells isolated from minced lungs or from umbilical veins have also been employed for experimental tumor therapy (Ojeifo et al., 2001; Rancourt et al., 1998).

In this study, we have used mouse embryonic endothelial progenitor cells for systemic cancer therapy for the first time. eEPCs can be easily propagated and genetically manipulated in culture, providing an unlimited source of cells with desired characteristics. eEPCs do not express MHC I antigens, are not susceptible to lysis by nonactivated NK cells, and survive and participate in tumor vessel formation in nonsyngeneic mice.

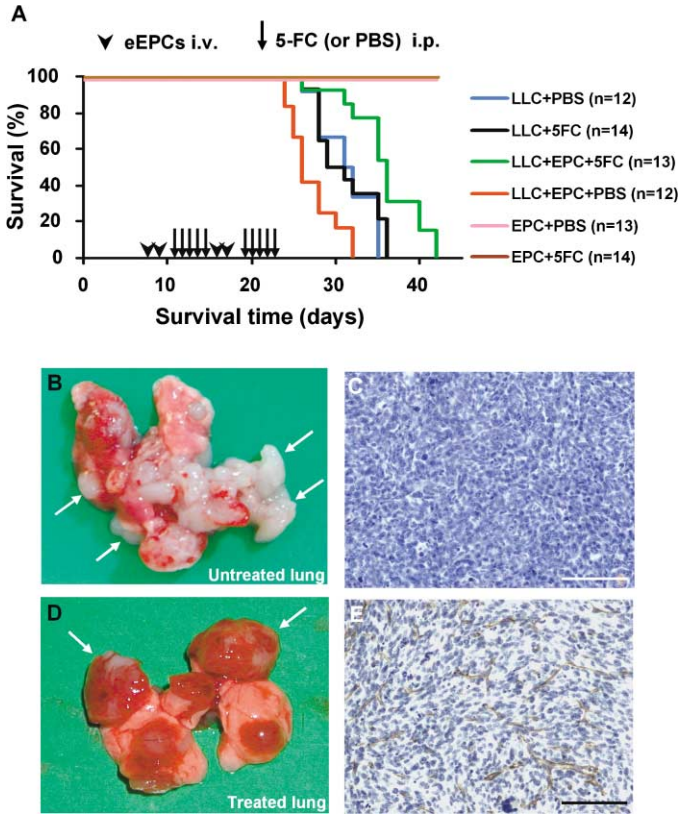

Figure 8. eEPC-CD engraftment coupled to 5-FC treatment prolongs life of mice with LLC pulmonary metastases by eradicating hypovascular tumors

A: 10- to 12-week-old male C57/BL/6 mice were injected via the tail vein with 5×10^5 LLC cells on day 0. After metastases were established, mice were given the first of two i.v. injections of 4×10^5 eEPC-CD cells spaced 48 hr apart. One day after the last inoculation of eEPC-CD, mice received 12.5 mg 5-FC in 600 μl PBS i.p. twice daily for 5 days. A second cycle of eEPC-CD followed by 5-FC was started on day 16. The treatment group (green line) received the therapy described above. Control groups received LLC cells and PBS (blue line), LLC cells and 5-FC (black line), LLC cells and eEPC-CD and PBS (red line), eEPC-CD and PBS (pink line), and eEPC-CD and 5-FC (brown line). Kaplan-Meier survival curves show a prolonged survival time of the metastasis-bearing mice treated with eEPC-CD and 5-FC (green line) compared to the metastasis-bearing control groups that did not receive eEPC-CD (blue and black lines; $p < 0.05$). Tumor-bearing mice that received eEPC-CD but no 5-FC (red line) survived shorter compared to the control groups (blue and black lines; $p < 0.05$). All non-tumor-bearing mice that had received eEPC-CDs survived (pink and brown lines). The numbers of animals (n) in each group are indicated.

B: Representative lung from the control group that received LLC cells and PBS only (blue line in **A**). Most of the metastases show only slight red coloration, indicating poor vascularization (arrows).

C: Histological analysis using an anti-CD31 antibody of lung metastases shown in **B** indicates that they contain few blood vessels.

D: Representative lung from the treatment group (eEPC-CD and 5-FC, green line in **A**). Metastases in the treatment group (arrows) are fewer but larger and well vascularized.

E: Surviving metastases are well vascularized. Histological analysis of a representative metastasis that escaped the cytotoxic effect of eEPC-CD shows numerous vessels. Endothelial cells were stained using an antibody against CD31. In both cases lungs were procured at the time when the mice appeared moribund. Scale bars represent 100 μm.

Thus, eEPCs from MHC-incompatible donors may, at least initially, be protected against cytotoxic T cells and NK cells after in vivo administration. This raises hopes for future engineering of EPCs for application as universal cellular vehicles independent of host/donor compatibility.

To further evaluate the therapeutic value of eEPCs, we thoroughly analyzed their biodistribution into normal organs and scrutinized transplanted mice for possible side effects. After tail vein injection into mice without tumors, eEPCs were sequestered at low density in the lung, spleen, and to a lesser extent the liver. The number of eEPCs sequestered in organs decreased with time. In this respect, eEPCs follow the fate of most cells injected i.v. (Pabst et al., 1987; Brown et al., 1995). Given the propensity of embryonic stem cells to form teratocarcinomas, it is important to note that eEPCs did not form tumors up to 3 months after subcutaneous or i.v. transplantation. The maturity of eEPCs as compared to embryonic stem cells may account for this. The low numbers of eEPCs found in the organs did not lead to toxic effects. This is further documented by the fact that survival rates were not affected in tumor-free control mice that received eEPC-CD or eEPC-CD and 5-FC (all animals, 13 and 14 mice, respectively, survived and showed no adverse effects).

Homing of eEPCs to lung tumors was very efficient: after two consecutive i.v. injections, 77% and 90% of all lung tumor nodules were targeted in the nonsyngeneic LM8 osteosarcoma and the LLC syngeneic metastasis models, respectively. Also, while eEPCs were sequestered in the healthy lung and were cleared over time if no metastases were present, eEPCs homed to and remained in hypovascular metastases. In both models of predominant lung tumors described here, the large numbers of eEPCs found in the lung metastases could be attributed to the combined effects of the high metastasis density in the lung and the fact that the eEPCs reach this organ first. Therefore, this approach might be best suited for the treatment of lung tumors. Targeting tumors in other organs may require injecting eEPCs into the appropriate afferent vessels. In addition, liver and kidney metastases in the LM8 model expressed less VEGF than lung metastases (Figures 4M–4O), suggesting that they were less hypoxic and thus less likely to recruit eEPCs.

This degree of homing is remarkable considering that it was achieved without prior bone marrow transplantation. Postirradiation bone marrow transplantation biases toward homing of exogenous EPCs by decreasing competition from endogenous EPCs (De Palma et al., 2003), by establishing a continuous source of bone marrow-derived exogenous EPCs, and by upregulating tumor angiogenesis (Sonveaux et al., 2003). Moreover, the need of lethal or sublethal myeloablation would severely limit the applicability of EPCs in the clinical setting. The independence of homing from bone marrow transplantation may be a major advantage of embryonic EPCs as compared to adult counterparts.

eEPCs also exhibited a remarkable specificity for metastases. 5 to 7 days after injection, eEPCs were found in low numbers in normal lung tissue, but they congregated densely in the metastases. The preferential homing of eEPCs into lung metastases does not reflect an unspecific sequestration into the lung. First, there was long-term accumulation of eEPCs at the metastases with scant eEPCs in the normal lung tissue. If homing of eEPCs was a passive event, one would expect a homogeneous distribution of eEPCs throughout normal and tumor tissue and a clearing

of eEPCs with time. Second, in contrast to eEPCs, mouse fibroblasts that have similar size to eEPCs did not show tumor-specific accumulation after i.v. injection. In support of these findings, we have previously shown using intravital microscopy that homing follows an active interaction between eEPCs and tumor vasculature with E- and P-selectin expressed on tumor cells mediating the initial eEPC recruitment step (Vajkoczy et al., 2003). We did not observe in these experiments that injected eEPCs obstructed tumor vessels. It is possible that the tumor microenvironment enhances survival and proliferation of sequestered eEPCs and thus contributes to eEPC accumulation within the metastases.

The lung metastases-bearing mice that received eEPCs survived a shorter time, suggesting an unwanted paracrine effect of eEPCs on tumor or tumor endothelial cells possibly due to production of VEGF or other growth factors. Consistent with this hypothesis, we find that eEPCs preferentially accumulate in the vicinity of hypoxic areas in the tumor and that hypoxia strongly upregulates VEGF expression in eEPCs. VEGF in turn can increase angiogenesis and also exert a proliferative and antiapoptotic effect both on tumor and tumor endothelial cells (Masood et al., 2001; Bachelder et al., 2001).

Intravenously injected eEPCs contributed long-term to tumor vasculature. The number of eEPC-containing vessels varied from metastasis to metastasis between 1% and 5% in the LLC model and between 4% and 7% in the LM8 model. Although many eEPCs had incorporated into tumor vessels, the majority of eEPCs were still found inside the tumor tissue. However, the number of eEPCs found in blood vessels rises dramatically if the eEPCs and the tumor cells are co-implanted simultaneously in subcutaneous locations. This observation reflects recent findings using ES-derived EPCs in tumor-induced angiogenesis models (Marchetti et al., 2002; Yurugi-Kobayashi et al., 2003). In these studies, no homing to tumors was detected, but ES-derived EPCs significantly contributed to tumor blood vessels if co-implanted with tumor cells. The eEPCs used in this study, isolated from day 7.5 mouse embryos, show efficient homing to angiogenic sites, suggesting a richer expression profile of cell-cell interaction receptors and chemotactic receptors. If eEPCs are administered i.v. in conditions of aggressive local angiogenesis, they probably cannot compete effectively with the local sprouting endothelium as well as with circulating endogenous EPCs. Therefore, their intrinsic ability to form de novo blood vessels in situ, as in the embryo, might be better manifested if eEPCs are present at early stages during neoangiogenesis. In our study, this limitation was not critical for therapeutic efficacy. Although the percentage of tumor blood vessels formed by eEPCs given i.v. was relatively low, the specific and efficient homing to metastases as opposed to normal tissues could be exploited for attacking the tumor.

To target metastases, we armed the eEPCs with the suicide gene CD/UPRT. eEPCs expressing CD/UPRT exhibited a significant bystander cytotoxic effect in vitro on both endothelial and tumor cells. Given systemically and followed by the prodrug 5-FC, eEPCs significantly prolonged the lifetime of mice with multiple established lung metastases. However, prolongation of survival was moderate and no cures were achieved. Several reasons may account for this result. First, eEPCs homed poorly to well-vascularized metastases, which subsequently continued to grow and killed the mice. On the other hand, the eEPCs' ability to home to poorly vascularized, hypoxic metastases may be one of their major advantages because hypoxic tumors are notoriously resistant to chemotherapy, radiation, and antiangiogenic therapies given as single modalities. Second, within the time frame of the treatment experiments, the eEPCs were predominantly found within the tumor tissue and not the tumor vasculature. This is consistent with recent findings that undifferentiated eEPCs deposited around subcutaneous tumors form clusters within the tumor, while eEPCs differentiated in vitro incorporate into tumor vessels after the same procedure (Yurugi-Kobayashi et al., 2003). Our tumor/eEPCs co-implantation experiments also show that eEPCs effectively incorporate into tumor vasculature only after prolonged time periods (3–4 weeks). Therefore, while immature eEPCs would be able to exert a bystander effect on tumor cells, they might kill only a few tumor endothelial cells. Third, homed eEPCs may enhance tumor growth until the suicide gene system is triggered. Tumor growth may be enhanced by increased vascularity due to eEPCs incorporating in tumor vessels. However, the number of eEPC-containing tumor vessels was too low to fully account for the observed lower survival rates of eEPC-injected tumor-bearing mice. Trophic factors produced by the large number of homed eEPCs may increase tumor growth. The VEGF produced in the homed eEPCs may augment angiogenesis and also exert a proliferative and antiapoptotic effect both on tumor and tumor endothelial cells (Shweiki et al., 1992; Masood et al., 2001; Bachelder et al., 2001). Fourth, suicide gene systems need time to kill bystander cells, because they first have to convert the prodrug to a cytotoxic compound. The CD/UPRT enzymatic system starts to kill bystander cells in significant numbers only after 3 days, a period long enough for the rapidly growing tumors to become too large to eradicate. Lastly, any cellular vehicle with a suicide gene system has the inherent disadvantage of destroying itself by the very same mechanism by which it kills tumor cells. Further studies will need to address these points.

In conclusion, intravenously delivered therapeutic embryonic endothelial progenitor cells target lung metastases, even in MHC I disparate hosts and do not form carcinomas. eEPCs show limited and transient engraftment efficiency in normal tissues, whereas they home and survive long-term within metastases, particularly if these are hypovascular and hypoxic. Further investigations will have to assess whether homing-associated molecules of tumor or stroma are differentially expressed in recruiting and nonrecruiting metastases and whether these differences can account for preferential recruitment. Future experiments will also aim to increase the efficacy of therapeutic eEPCs in combination regimes designed to target well-vascularized metastases by chemo- or anti-angiogenic therapy in parallel.

Experimental procedures

Cell culture

eEPCs were isolated from mouse embryos at day 7.5 to 7.8 of development and propagated as primary cell lines as described (Hatzopoulos et al., 1998). The murine osteosarcoma cell line LM8 was grown in MEM α medium supplemented with 10% heat-inactivated fetal calf serum (FCS). Lewis lung carcinoma cells 3LL-D122 were grown in DMEM with 1 mM sodium pyruvate supplemented with 10% FCS. bEnd5 cells were maintained in DMEM medium supplemented with 10% FCS and 5 μM β-mercaptoethanol. For fibroblast cell culture, skin from C57BL/6J mice was minced and placed in culture dishes with DMEM, 15% FCS, and 5 μM β-mercaptoethanol. Outgrowing adherent cells were passaged repeatedly. All culture media were supplemented with 2 mM glutamine, 2 mM nonessential amino acids, 100 U/ml

penicillin, and 100 μg/ml streptomycin. Tissue culture materials were obtained from Life Technologies Inc. (Eggenstein, Germany).

Plasmid constructs

The pCIneo-CD/UPRT vector expressing the suicide gene was obtained from Transgene S.A. (Strasbourg, France). The vector pCI-neo (Promega, Mannheim, Germany) was used as empty vector control. The pPGK-EGFP plasmid was generated from pPGK-neo (PGK, phosphoglycerate kinase promoter) by substituting the neomycin resistance gene with EGFP (Clontech, Heidelberg, Germany).

Cell transfection

Either pCIneo-CD/UPRT, pCI-neo, or pPGK-EGFP were transfected into eEPCs using Lipofect according to the manufacturer's instructions (Stratagene, La Jolla, CA), and stably transfected cells were selected yielding eEPC-CD, eEPC-mock, and eEPC-EGFP, respectively.

Flow cytometry

Suspended eEPCs, NIH 3T3 cells, T cells, and primary mast cells (kindly provided by Dr. Hültner, GSF, Germany) were incubated with 10 μg/ml rat pan anti-mouse MHC I antibody (TIB 126; ATCC, Manassas, VA) or purified rat IgG1 (BD Pharmingen, San Diego, CA) in FACS buffer (1% BSA and 0.1% NaN_3 in phosphate-buffered saline [PBS]) for 30 min on ice. Subsequently, eEPCs were washed twice and incubated with 10 μg/ml phycoerythrin (PE)-conjugated anti-rat IgG (Dianova, Hamburg, Germany) in FACS buffer and 5% mouse serum for 30 min. Analysis was performed on a FACSCalibur flow cytometer using CellQuest software (Becton Dickinson, San Jose, CA).

NK cell cytotoxicity assays

NK cell cytotoxicity assays were carried out as described (Chan et al., 2001). Briefly, splenocytes were depleted of $CD4^+$ and $CD8^+$ cells by complement lysis and used in a standard ^{51}Cr-release assay against YAC-1 (Kiessling et al., 1975), RMA/S (Ljunggren and Karre, 1985), and T15B (an eEPC line) cells as targets. Target cells were labeled with ^{51}Cr (100 mCi; Amersham Biosciences, Freiburg, Germany) for 1 hr at 37°C. Cells were washed and incubated with NK effectors at effector (E):target (T) ratios as indicated. After 4 hr at 37°C, the cell-free supernatants were transferred to a γ counter to determine ^{51}Cr release. Spontaneous cell lysis and maximum cell lysis were measured using 10^4 cells in medium alone and in 1% Triton X-100, respectively. Percentage of specific lysis was calculated with the formula: % sample specific lysis = [(sample counts − spontaneous counts)/(maximum counts − spontaneous counts)] × 100%.

Assessment of biodistribution

The chelating ligand p-SCN-*mx*-DTPA (diethylenetriaminepenta-acetic acid) was coupled to LDL, creating a thiourea bond between the reactive SCN group of the chelator and a primary amine of the protein (in HEPES buffer [pH 7.9]). After purification (using size exclusion HPLC) and buffer exchange (acetate buffer [pH 5.0]), the labeling was performed with 60 MBq of ^{111}In. 30 MBq of the product ^{111}In-DTPA-LDL was isolated using size exclusion HPLC (purity > 98%). eEPCs were incubated with ^{111}In-DTPA-LDL for 4 hr at 37°C in serum-free medium. Cells (^{111}In-LDL-eEPCs) were washed and resuspended in serum-free medium. 6- to 8-week-old C3H male mice received 4×10^5 ^{111}In-LDL-eEPCs via tail vein injection. Mice were killed on day 2 (n = 3) and on day 5 (n = 3) after eEPC injection. Blood was aspirated by intracardiac puncture and the femurs and solid organs were procured. Samples were analyzed using a γ counter. Samples obtained from noninjected mice served as background control. To assess the biodistribution of eEPCs into solid organs by immunohistochemistry and into bone marrow by FACS analysis, 4×10^5 eEPC-EGFP cells were tail vein injected into C3H mice (n = 3). Noninjected mice (n = 3) were used as control. Solid organs were procured 2 days after the eEPC injection and analyzed using an anti-EGFP antibody for immunohistochemistry as described below. Bone marrow devoid of erythrocytes was analyzed by FACS analysis measuring forward scatter and EGFP fluorescence.

Assessment of homing

Either LM8 cells (2×10^5 per mouse) or LLC-D122 cells (5×10^5 per mouse) were injected into the tail vein of 8 C3H and 5 C57/BL/6 mice, respectively. Fourteen days later, the mice were given either one i.v. injection of 4×10^5 eEPC-EGFP cells or two such i.v. injections spaced 3 days apart. The mice were euthanized 5 to 7 days later. Tumor-bearing mice not transplanted with eEPC-EGFP cells (n = 5), as well as tumor-free mice that received the same number of eEPC-EGFP cells as the experimental groups (n = 5), were used as controls. Organs were removed and processed for immunohistochemical analysis as described below. To compare unspecific sequestration of cells with specific homing of eEPCs, 2 C57/BL/6 mice carrying established LLC pulmonary metastases were injected i.v. with 4×10^5 DiI-labeled skin fibroblasts from C57/BL/6 mice, while 3 tumor-bearing mice received the same number of DiI-labeled eEPCs. Lungs were procured 2 days after cell injection, snap-frozen, cryosectioned, and microscopically examined for DiI-fluorescence. To determine the long-term fate of eEPCs in tumors after homing, mice were injected with 4×10^5 DiI-labeled eEPCs per mouse via tail vein 9 days after LLC (n = 5) or LM8 (n = 3) injection. Organs were removed 14 to 17 days (LLC) or 10 days (LM8) after eEPC injection and snap frozen for further analysis. Tumor blood vessels were visualized after lectin or collagen IV staining as described below.

Immunofluorescence microscopy and lectin binding

Serial frozen sections were examined. DiI-labeled eEPCs were detected without further manipulations. For VEGF detection, we used 2 μg/ml rabbit anti-VEGF antibody (Santa Cruz Biotechnology, Santa Cruz, CA), followed by 2 μg/ml goat-anti-rabbit Cy3-conjugated IgG (Dianova). The anti-collagen IV rabbit antiserum was a kind gift of Dr. R. Timpl (MPI, Germany) and was used in 1:600 dilution followed by 3 μg/ml goat-anti-rabbit FITC-conjugated IgG (Dianova). Perfused blood vessels were visualized by injection of 200 μl of 550 μg/ml Helix Pomatia lectin (HPA) coupled with FITC (SIGMA, Steinheim, Germany) via the tail vein 5 min prior to organ isolation. FITC-labeled GSL I-isolectin B_4 (Vector Laboratories, Burlingame, CA) at a concentration of 150 μg/ml was used to detect mature endothelial cells. Hematoxylin or hematoxylin/eosin (H&E) were used for subsequent counterstaining.

Immunohistochemistry

Organs were fixed with buffered 3.7% formaldehyde solution, embedded in paraffin, and serially cut into 5 μm thick sections. Deparaffinized and rehydrated sections were either microwaved in citrate acid buffer (0.01 M, pH 6.0) or digested with proteinase K (DAKO, Hamburg, Germany) to demask antigens. Endogenous peroxidase was blocked with 3% H_2O_2, endogenous biotin activity by the biotin/avidin blocking system (DAKO), and unspecific antibody binding by 1% bovine serum albumin (BSA, Serva, Heidelberg, Germany) and 10% normal goat serum (DAKO). Slides were incubated overnight at 4°C with rabbit anti-EGFP (5 μg/ml in 0.1% Triton; Molecular Probes), rabbit anti-VEGF (2 μg/ml, Santa Cruz), and biotinylated rat anti-CD31 (6 μg/ml; DPC Biermann, Bad Nauheim, Germany). Peroxidase-conjugated goat anti-rabbit IgG (DAKO) was used as secondary antibody to detect EGFP and VEGF, while peroxidase-conjugated avidin/biotin complexes (DAKO) were employed for the detection of CD31.

Hypoxia detection

To detect tumor hypoxia in vivo, we injected pimonidazol (Hypoxyprobe-1, Chemicon International, Temecula, CA) at a dose of 60 mg/kg body weight via tail vein into mice 1 hr prior to organ isolation. Serial frozen sections were incubated with anti-pimonidazol Hypoxyprobe-1 Mab1 (Chemicon) diluted 1:50 followed by RPE-conjugated goat anti-mouse IgG1 $F(ab')_2$ (Southern Biotech, Birmingham, AL).

VEGF detection

eEPCs were cultured under normoxic (21% O_2) and hypoxic (2% O_2) conditions for 1 to 24 hr. The protocol for detection of VEGF and aldolase transcripts by RT-PCR has been described (Vajkoczy et al., 2003). VEGF protein was analyzed by immunoprecipitation followed by Western blotting using standard protocols.

Determination of cell death in vitro

Cell death was measured by the MTT [3-(4,5-dimethyl-2-thiazolyl)-2,5-diphenyl-2H-tetrazolium bromide] assay as described (Beltinger et al., 2002).

Bystander effect assays

eEPC-CD cells were mixed with LM8 or with bEnd5 cells in ratios of 0%, 1.6%, 3.2%, 6.3%, 12.5%, 25%, 50%, and 100%. The mixtures were plated

in 96-well plates at a density of 1×10^3 per well and allowed to attach overnight. Cells were then treated with medium alone (control) or with 1 mM 5-FC for 5 days and cell death was measured using the MTT assay.

In vivo survival experiments

10- to 12-week-old male C57/BL/6 mice were injected intravenously with 5×10^5 3LL-D122 cells and randomized to 4 groups ($n = 15$ per group). On day 8, two groups of mice were given the first of two intravenous injections of 4×10^5 eEPC-CD cells in 400 μl PBS spaced 48 hr apart. Starting 2 days after the last inoculation of eEPC-CD, either 12.5 mg 5-FC (SIGMA) in 600 μl PBS or the same volume of PBS were injected intraperitoneally twice daily for 5 days. This cycle of eEPC-CD administration followed by 5-FC injections was repeated once. Two additional groups of mice not transplanted with 3LL-D122 tumors received eEPC-CD cells i.v. as above, followed by administration of 5-FC or PBS for 5 days ($n = 15$). Tumor-bearing mice were monitored daily and sacrificed when appearing moribund as determined by a blinded observer. Surviving mice that received only eEPC-CD cells were killed 3 months later. Organs were removed and processed for histological analysis as described above. All animal work was performed in accordance with state guidelines for animal care and use.

Statistical analysis

Survival data were analyzed by Kaplan-Meier estimator analysis and compared using the Kruskal-Wallis Test for multiple comparisons and the Mann-Whitney Test for single comparisons. Values of $p < 0.05$ were considered significant.

Acknowledgments

We thank L. Eisenbach for 3LL-D122 cells, B. Engelhardt for bEnd5 cells, C. Matuschek for helpful discussions, and M. Herbst and M. Semisch for excellent technical assistance. This work was supported by grants from the IZKF Ulm and the Wilhelm Sander-Stiftung to C.B. and the DFG grant HA2983 of the Priority Program "Angiogenesis" SPP1069 and the German Human Genome Project grant 9907 to A.K.H.

Received: June 27, 2003
Revised: February 19, 2004
Accepted: March 15, 2004
Published: May 17, 2004

References

Asahara, T., Murohara, T., Sullivan, A., Silver, M., van der Zee, R., Li, T., Witzenbichler, B., Schatteman, G., and Isner, J.M. (1997). Isolation of putative progenitor endothelial cells for angiogenesis. Science *275*, 964–967.

Asahara, T., Masuda, H., Takahashi, T., Kalka, C., Pastore, C., Silver, M., Kearne, M., Magner, M., and Isner, J.M. (1999). Bone marrow origin of endothelial progenitor cells responsible for postnatal vasculogenesis in physiological and pathological neovascularization. Circ. Res. *85*, 221–228.

Bachelder, R.E., Crago, A., Chung, J., Wendt, M.A., Shaw, L.M., Robinson, G., and Mercurio, A.M. (2001). Vascular endothelial growth factor is an autocrine survival factor for neuropilin-expressing breast carcinoma cells. Cancer Res. *61*, 5736–5740.

Beltinger, C., Fulda, S., Walczak, H., and Debatin, K.M. (2002). TRAIL enhances thymidine kinase/ganciclovir gene therapy of neuroblastoma cells. Cancer Gene Ther. *9*, 372–381.

Brown, G.M., Brown, D.M., Donaldson, K., Drost, E., and MacNee, W. (1995). Neutrophil sequestration in rat lungs. Thorax *50*, 661–667.

Chan, G., Hanke, T., and Fischer, K.D. (2001). Vav-1 regulates NK T cell development and NK cell cytotoxicity. Eur. J. Immunol. *31*, 2403–2410.

Chung-Faye, G.A., Chen, M.J., Green, N.K., Burton, A., Anderson, D., Mautner, V., Searle, P.F., and Kerr, D.J. (2001). In vivo gene therapy for colon cancer using adenovirus-mediated transfer of the fusion gene cytosine deaminase and uracil phosphoribosyltransferase. Gene Ther. *8*, 1547–1554.

Davidoff, A.M., Ng, C.Y., Brown, P., Leary, M.A., Spurbeck, W.W., Zhou, J., Horwitz, E., Vanin, E.F., and Nienhuis, A.W. (2001). Bone marrow-derived cells contribute to tumor neovasculature and, when modified to express an angiogenesis inhibitor, can restrict tumor growth in mice. Clin. Cancer Res. *7*, 2870–2879.

De Palma, M., Venneri, M.A., Roca, C., and Naldini, L. (2003). Targeting exogenous genes to tumor angiogenesis by transplantation of genetically modified hematopoietic stem cells. Nat. Med. *9*, 789–795.

Ferrari, N., Glod, J., Lee, J., Kobiler, D., and Fine, H.A. (2003). Bone marrow-derived, endothelial progenitor-like cells as angiogenesis-selective gene-targeting vectors. Gene Ther. *10*, 647–656.

Gehling, U.M., Ergun, S., Schumacher, U., Wagener, C., Pantel, K., Otte, M., Schuch, G., Schafhausen, P., Mende, T., Kilic, N., et al. (2000). In vitro differentiation of endothelial cells from AC133-positive progenitor cells. Blood *95*, 3106–3112.

Gomez-Navarro, J., Contreras, J.L., Arafat, W., Jiang, X.L., Krisky, D., Oligino, T., Marconi, P., Hubbard, B., Glorioso, J.C., Curiel, D.T., and Thomas, J.M. (2000). Genetically modified CD34+ cells as cellular vehicles for gene delivery into areas of angiogenesis in a rhesus model. Gene Ther. *7*, 43–52.

Hanahan, D., and Folkman, J. (1996). Patterns and emerging mechanisms of the angiogenic switch during tumorigenesis. Cell *86*, 353–364.

Hatzopoulos, A.K., Folkman, J., Vasile, E., Eiselen, G.K., and Rosenberg, R.D. (1998). Isolation and characterization of endothelial progenitor cells from mouse embryos. Development *125*, 1457–1468.

Huber, B.E., Austin, E.A., Richards, C.A., Davis, S.T., and Good, S.S. (1994). Metabolism of 5-fluorocytosine to 5-fluorouracil in human colorectal tumor cells transduced with the cytosine deaminase gene: significant antitumor effects when only a small percentage of tumor cells express cytosine deaminase. Proc. Natl. Acad. Sci. USA *91*, 8302–8306.

Kiessling, R., Klein, E., Pross, H., and Wigzell, H. (1975). Natural killer cells in the mouse. II. Cytotoxic cells with specificity for mouse Moloney leukemia cells. Characteristics of the killer cell. Eur. J. Immunol. *5*, 117–121.

Levenberg, S., Golub, J.S., Amit, M., Itskovitz-Eldor, J., and Langer, R. (2002). Endothelial cells derived from human embryonic stem cells. Proc. Natl. Acad. Sci. USA *99*, 4391–4396.

Ljunggren, H.G., and Karre, K. (1985). Host resistance directed selectively against H-2-deficient lymphoma variants. Analysis of the mechanism. J. Exp. Med. *162*, 1745–1759.

Lyden, D., Hattori, K., Dias, S., Costa, C., Blaikie, P., Butros, L., Chadburn, A., Heissig, B., Marks, W., Witte, L., et al. (2001). Impaired recruitment of bone-marrow-derived endothelial and hematopoietic precursor cells blocks tumor angiogenesis and growth. Nat. Med. *7*, 1194–1201.

Marchetti, S., Gimond, C., Iljin, K., Bourcier, C., Alitalo, K., Pouyssegur, J., and Pages, G. (2002). Endothelial cells genetically selected from differentiating mouse embryonic stem cells incorporate at sites of neovascularization in vivo. J. Cell Sci. *115*, 2075–2085.

Masood, R., Cai, J., Zheng, T., Smith, D.L., Hinton, D.R., and Gill, P.S. (2001). Vascular endothelial growth factor (VEGF) is an autocrine growth factor for VEGF receptor-positive human tumors. Blood *98*, 1904–1913.

Ojeifo, J.O., Lee, H.R., Rezza, P., Su, N., and Zwiebel, J.A. (2001). Endothelial cell-based systemic gene therapy of metastatic melanoma. Cancer Gene Ther. *8*, 636–648.

Pabst, R., Binns, R.M., Licence, S.T., and Peter, M. (1987). Evidence of a selective major vascular marginal pool of lymphocytes in the lung. Am. Rev. Respir. Dis. *136*, 1213–1218.

Patterson, C. (2003). The Ponzo effect: endothelial progenitor cells appear on the horizon. Circulation *107*, 2995–2997.

Peichev, M., Naiyer, A.J., Pereira, D., Zhu, Z., Lane, W.J., Williams, M., Oz, M.C., Hicklin, D.J., Witte, L., Moore, M.A., and Rafii, S. (2000). Expression of VEGFR-2 and AC133 by circulating human CD34(+) cells identifies a population of functional endothelial precursors. Blood *95*, 952–958.

Rafii, S., and Lyden, D. (2003). Therapeutic stem and progenitor cell transplantation for organ vascularization and regeneration. Nat. Med. *9*, 702–712.

Rancourt, C., Robertson, M.W., 3rd, Wang, M., Goldman, C.K., Kelly, J.F., Alvarez, R.D., Siegal, G.P., and Curiel, D.T. (1998). Endothelial cell vehicles for delivery of cytotoxic genes as a gene therapy approach for carcinoma of the ovary. Clin. Cancer Res. *4*, 265–270.

Reyes, M., Dudek, A., Jahagirdar, B., Koodie, L., Marker, P.H., and Verfaillie, C.M. (2002). Origin of endothelial progenitors in human postnatal bone marrow. J. Clin. Invest. *109*, 337–346.

Rogers, B.E., Franano, F.N., Duncan, J.R., Edwards, W.B., Anderson, C.J., Connett, J.M., and Welch, M.J. (1995). Identification of metabolites of 111In-diethylenetriaminepentaacetic acid-monoclonal antibodies and antibody fragments in vivo. Cancer Res. *55*, 5714–5720.

Shi, Q., Rafii, S., Wu, M.H., Wijelath, E.S., Yu, C., Ishida, A., Fujita, Y., Kothari, S., Mohle, R., Sauvage, L.R., et al. (1998). Evidence for circulating bone marrow-derived endothelial cells. Blood *92*, 362–367.

Shweiki, D., Itin, A., Soffer, D., and Keshet, E. (1992). Vascular endothelial growth factor induced by hypoxia may mediate hypoxia-initiated angiogenesis. Nature *359*, 843–845.

Sonveaux, P., Brouet, A., Havaux, X., Gregoire, V., Dessy, C., Balligand, J.L., and Feron, O. (2003). Irradiation-induced angiogenesis through the up-regulation of the nitric oxide pathway: implications for tumor radiotherapy. Cancer Res. *63*, 1012–1019.

Vajkoczy, P., Blum, S., Lamparter, M., Mailhammer, R., Erber, R., Engelhardt, B., Vestweber, D., and Hatzopoulos, A.K. (2003). Multistep nature of microvascular recruitment of ex vivo-expanded embryonic endothelial progenitor cells during tumor angiogenesis. J. Exp. Med. *197*, 1755–1765.

Virgolini, I., Angelberger, P., Li, S.R., Koller, F., Koller, E., Pidlich, J., Lupattelli, G., and Sinzinger, H. (1991). Indium-111-labeled low-density lipoprotein binds with higher affinity to the human liver as compared to iodine-123-low-density-labeled lipoprotein. J. Nucl. Med. *32*, 2132–2138.

Yurugi-Kobayashi, T., Itoh, H., Yamashita, J., Yamahara, K., Hirai, H., Kobayashi, T., Ogawa, M., Nishikawa, S., Nishikawa, S., and Nakao, K. (2003). Effective contribution of transplanted vascular progenitor cells derived from embryonic stem cells to adult neovascularization in proper differentiation stage. Blood *101*, 2675–2678.